ACS Sustainable Chemistry & Engineering

Research Article

Cite This: ACS Sustainable Chem. Eng. 2018, 6, 14480−14489

pubs.acs.org/journal/ascecg

Valorization of Wheat Straw Using a Recyclable Hydrotrope at Low Temperatures (≤90 °C)

Qianli Ma,[†,‡] Junjun Zhu,[‡,§] Rolland Gleisner,[‡] Rendang Yang,[†] and J.Y. Zhu*[,‡]

[†]State Key Lab Pulp and Paper Engineering, South China University of Technology, 381 Wushan Road, Guangzhou 510630, China

[‡]USDA Forest Service, Forest Products Laboratory, One Gifford Pinchot Dr., Madison, Wisconsin 53726, United States

[§]College of Chemical Engineering, Nanjing Forestry University, 159 Longpan Road, Nanjing 210037, China

Supporting Information

ABSTRACT: This study evaluated the potential of an acid hydrotropic process at low temperatures for on-farm valorization of wheat straw by producing ligocellulosic nanofibrils (LCNFs), lignin nanoparticles (LNPs), and furfural. *p*-Toluenesulfonic acid (*p*-TsOH) was used to fractionate wheat straw under a range of conditions below 90 °C at low to moderate concentrations, between 15 and 60 wt %, for up to 2 h. *p*-TsOH fractionated wheat straw into a cellulose-rich water-insoluble solid (WIS) fraction and a spent liquor stream that contained dissolved lignin and xylan. Various degrees of delignification and hemicellulose dissolution were obtained and were correlated with a combined delignification factor (CDF) and a combined hydrolysis factor (CHF), respectively. A low *p*-TsOH concentration of 15 wt % can be used to obtain the desired degree of delignification for producing LCNFs directly from wheat straw. Films made of wheat straw LCNFs, with lignin contents of 12−22%, had excellent mechanical properties, with specific tensile strength over 120 kN·m/kg. The dissolved xylan in the spent liquor was directly dehydrated into furfural catalyzed by the *p*-TsOH in the spent liquor without an additional catalyst. The dissolved lignin was easily precipitated as LNPs through dilution using water. *p*-TsOH, as a solid catalyst, can be reused after the steps of lignin precipitation, reconcentration, and dehydration of xylose into furfural. The low-temperature fractionation process could substantially reduce capital and operating costs for on-farm applications.

KEYWORDS: *Wheat straw, Hydrotropic fractionation, Low temperature, Lignocellulose nanofibrils, Lignin nanoparticles*

INTRODUCTION

Wheat straw is a renewable and abundant agricultural resource that can be valorized for sustainable economic development in rural areas. Approximately 30−40 million dry tons of wheat straw can be collected in the United States annually at a price of $60/dry ton, substantially lower than the price of corn stover at $90/dry ton or other energy crops, such as switchgrass at $95−130/dry ton.[1] Europe and Southeast Asia are the largest producers of wheat, and therefore, wheat straw with an annual straw production of approximately 200 million dry tons for each.[2] China alone reported a wheat straw production of 175 million dry tons in 2015.[3] Currently, this abundant renewable resource is not well utilized and, in fact, has created a disposal problem in many regions of the world using primitive methods, such as open field-burning.[2,4] Traditional utilization of wheat straw includes papermaking using acidic sulfite pulping, animal feed and bedding, and fertilizer or soil conditioner.[5−8] The economics, the sizes of these markets compared with the available amount of wheat straw, and the environmental concerns about the processing methods used for some of these traditional utilization methods[2,5] demand exploration of new and high-value utilization options for wheat straw. Attempts have been made to use wheat straw as an energy source by combustion in power plants.[9,10] The inorganic species present in wheat straw tend to have reduced melting points[11] and lead to sintering or formation of fouling that substantially limits its use in boilers.[12]

Producing nanomaterials from lignocelluloses can be a potentially viable and high-value utilization of wheat straw, especially if this can be done on-farm to reduce issues associated with straw storage and supply chain. A few studies have been carried out on producing lignocellulosic nanofibrils (LCNFs) directly from wheat straw.[13−16] Despite the low lignin content of wheat straw, a chemical treatment step to partially solubilize some chemical components such as lignin and hemicelluloses is necessary to facilitate and reduce mechanical energy input[17] for nanofibrillation. Conventional mineral acid prehydrolysis cannot achieve the desired levels of delignification but rather condenses lignin, which can make

Received: July 3, 2018
Revised: September 20, 2018
Published: October 11, 2018

DOI: 10.1021/acssuschemeng.8b03135
ACS Sustainable Chem. Eng. 2018, 6, 14480−14489

Table 1. Chemical Compositions of *p*-TsOH-Fractionated Wheat Straw Samples under Different Treatment Conditions[a]

		WIS					spent liquor				
sample label[b]	solids yield (%)	glucan (%)	xylan (%)	arabinan (%)	ash (%)	lignin (%)	glucose (g/L)	xylose (g/L)	formic acid (g/L)	acetic acid (g/L)	furfural[c] (g/L)
untreated wheat straw	100	40.8	24.5	2.3	5.1	20.4					
P20T40t20	94.65	41.4 (95.9)	22.9 (88.3)	2.3 (95.9)	5.3 (97.7)	20.7 (96.2)	ND	0.06 (0.4)	0	0.05	ND
P20T50t20	93.30	39.5 (90.2)	21.8 (82.8)	2.1 (87.0)	5.5 (100.4)	19.9 (91.2)	ND	0.06 (0.4)	0	0.07	ND
P20T60t20	89.75	38.3 (84.2)	21.5 (78.5)	1.7 (66.9)	6.4 (111.9)	19.5 (85.9)	ND	0.09 (0.4)	0	0.15	ND
P25T60t30	87.31	41.1 (88.0)	22.0 (78.3)	1.6 (60.9)	5.2 (87.7)	19.0 (81.7)	ND	0.13 (0.6)	0	0.25	ND
P25T60t30R	87.31	41.7 (89.2)	22.9 (81.4)	1.6 (61.1)	6.1 (103.7)	19.8 (85.1)					
P35T60t30	80.50	43.2 (85.2)	20.5 (67.4)	0.7 (23.6)	8.2 (128.1)	20.7 (81.8)	ND	0.13 (1.0)	0	0.38	ND
P35T60t60	75.50	45.4 (84.0)	17.9 (55.2)	0.3 (10.8)	7.1 (104.2)	19.1 (70.7)	ND	0.23 (1.8)	0	0.57	ND
P40T70t60	67.07	48.3 (79.4)	14.9 (40.7)	0.2 (5.8)	9.0 (117.4)	17.8 (58.5)	ND	2.34 (19.6)	0.10	0.81	ND
P40T80t60	66.04	54.7 (88.6)	13.4 (36.1)	ND	8.9 (114.1)	16.9 (54.8)	0.07 (0.1)	5.59 (45.1)	0.11	0.81	0.06 (0.6)
P40T80t60R	66.04	52.5 (84.9)	13.3 (35.9)	ND	7.6 (97.2)	17.2 (55.8)					
P40T80t90	58.30	57.7 (80.4)	12.0 (27.9)	ND	9.2 (104.0)	16.3 (46.8)	0.15 (0.4)	6.25 (50.0)	0.15	0.88	0.05 (0.5)
P40T80t120	62.32	56.3 (88.1)	11.7 (30.5)	ND	9.2 (111.8)	15.8 (48.4)	0.22 (0.8)	7.04 (55.8)	0.12	0.91	0.06 (0.6)
P50T80t60	57.16	55.1 (77.1)	11.4 (26.5)	ND	9.5 (105.5)	14.4 (40.5)	0.20 (0.6)	6.56 (49.8)	0.15	0.87	0.06 (0.7)
P50T80t90	55.97	59.0 (80.9)	10.9 (24.9)	ND	9.2 (99.8)	14.0 (38.6)	0.26 (0.8)	6.88 (51.7)	0.14	0.89	0.07 (0.8)
P60T80t60	55.04	62.1 (83.8)	10.0 (22.4)	ND	8.5 (91.2)	11.2 (30.3)	0.37 (1.6)	7.74 (59.1)	0.14	0.94	0.17 (1.9)
P60T80t90	54.97	59.3 (79.9)	8.5 (19.1)	ND	10.1 (108.4)	14.0 (37.9)	0.47 (2.2)	8.13 (62.9)	0.14	0.88	0.26 (3.0)
					Large Batches for LCNF						
P15T90t120	70.22	49.5 (85.2)	9.0 (25.8)	ND	8.6 (117.5)	22.0 (75.9)	0.88 (3.9)	8.42 (60.5)	0.17	0.90	0.05 (10.1)
P25T90t120	62.73	53.5 (82.2)	9.0 (23.3)	ND	9.4 (114.8)	17.0 (52.4)	1.17 (5.2)	9.60 (68.9)	0.66	0.99	0.10 (11.2)
P35T90t120	56.21	58.1 (80.0)	9.4 (21.6)	ND	10.5 (114.9)	12.4 (34.2)	1.35 (6.0)	10.77 (77.3)	0.95	1.12	0.06 (12.5)

[a]Numbers in parentheses are component yields based on the component in the untreated wheat straw. [b]PxxTyytzz stands for *p*-TsOH concentration in wt %, reaction temperature in °C, and duration in min. R stands for replicate run. [c]Yields are based on the xylan content in untreated wheat straw. ND stands for not detectable.

DOI: 10.1021/acssuschemeng.8b03135
ACS Sustainable Chem. Eng. 2018, 6, 14480−14489

subsequent fibrillation difficult. Furthermore, mineral acid hydrolysis can substantially degrade cellulose, which can affect the strength of cellulose nanomaterials. Existing studies on LCNF production from wheat straw use high temperature (i.e., high pressure[16]) or pulping processes,[15] both of which are not suitable for on-farm LCNF production due to high capital and energy costs. Some of the studies ignore the utilization of lignin and dissolved hemicelluloses,[13,14] both of which are major components of wheat straw and can negatively impact process economics.

Another lignocellulosic-based nanomaterial, lignin nanoparticles (LNPs), has attracted great attention recently for a variety of applications, such as being copolymers in rubber[18] and composites,[19] surfactants in pickering emulsion,[20,21] and vehicles for drug delivery.[22,23] Current production of LNPs is mainly from the technical lignin, which is available in large quantities but requires solvents, such as ethylene glycol,[24] THF,[25] DMF,[20,21,26] and acetone,[27] to solubilize. Most of these solvents are not environmentally friendly, and the cost of solvent recovery negatively affects process economics.

The objective of this study is to demonstrate the production of wheat straw-based nanomaterials, such as LCNFs and LNPs, at low temperatures (i.e., below the boiling point of water), with the potential of low capital costs and easy recovery of both chemicals and lignin for on-farm applications. By using an acid hydrotrope,[28] *p*-toluenesulfonic acid (*p*-TsOH), wheat straw can be fractionated at low temperatures (i.e., below the boiling point of water) into a cellulosic-rich water-insoluble solid (WIS) fraction, that can be used to produce LCNFs, and a liquor stream, that primarily contains dissolved lignin, xylan, and the catalyst *p*-TsOH. The dissolved lignin can be precipitated as LNPs simply by diluting the liquor with water to below the minimum hydrotrope concentration (MHC) of 11.5%. *p*-TsOH as a solid catalyst can then be reused or recycled through concentration. The dissolved xylan in the spent liquor can be dehydrated into furfural using *p*-TsOH in the spent liquor without additional catalysts at elevated temperatures. *p*-TsOH, as an acid, does not remove silica (ash) from wheat straw, which not only increases material yields of WIS but also eliminates potential equipment fouling and other processing problems downstream. Comparing existing fractionation processes (carried out at high temperatures and pressures using chemicals, such as organic solvents,[29,30] ionic liquids,[31−33] supercritical treatment,[34] and sulfite[35]) with this low-temperature (no pressure vessels required) and simple chemistry (using only one catalyst to valorize all components of wheat straw) process, the present hydrotropic process has substantial advantages for on-farm applications.

MATERIALS AND METHODS

Materials. *p*-TsOH of ACS reagent grade was purchased from Sigma-Aldrich (St. Louis, MO). All chemicals were used as received.

Wheat straw was hammer milled using a 4.8 mm screen. The hammer milled wheat straw was first soaked in deionized (DI) water and washed three times at 2% consistency at room temperature to wash away dirt from harvesting. The resultant slurries were then vacuum dewatered and air-dried to approximately 10% water content. For actual on-farm operations, water usage for washing can be substantially reduced by using efficient countercurrent washing systems. Furthermore, the washed water can be easily recycled and reused simply by precipitating the washed out dirt. The washed wet wheat straw solids will be directly used for fractionation without drying. The moisture remaining in the washed wet straw reduced the water application for the subsequent fractionation step.

***p*-TsOH Fractionation.** Aqueous *p*-TsOH solutions of 15−60 wt % concentrations were prepared in conical flasks by solubilizing desired amounts of *p*-TsOH in 100 mL of DI water. To facilitate solubilization of *p*-TsOH, each flask was placed on a temperature-controlled shaker (Model 4450, Thermo Scientific, Waltham, MA, USA) at 200 rpm. A 5-g (ovendry weight) sample of the air-dried wheat straw was placed into 100 g of prepared *p*-TsOH solution with continuous shaking at a designed temperature and for a predetermined period of time. The fractionation runs were labeled as PxxTyytzz to represent the *p*-TsOH concentration of *xx* wt % at *yy* °C for *zz* min, as listed in Table 1. At the end of each fractionation reaction, the spent *p*-TsOH liquor was separated through filtration using filter paper under vacuum. The solids were washed three times with DI water. Recovery of *p*-TsOH from washing was over 95%. The filtrate was diluted using DI water to 10 wt % *p*-TsOH concentration, below the MHC of *p*-TsOH. The washed WISs were analyzed for chemical compositions. The WIS from three separate large (50 g of wheat straw) fractionation runs, as listed in Table 1, were used for producing three separate batches of LCNFs through disk milling, as schematically shown in Figure 1 and further discussed below.

Figure 1. A schematic flow diagram showing fractionation of wheat straw and productions of LCNFs and LNPs.

Mechanical Fibrillation of WISs. The WISs from the three large runs were mechanically fibrillated using a disk grinder, Super-MassColloider (SMC) (MKZA 6-2; Disk model, MDGA 6-80#; Masuko Sangyo Co., Ltd., Japan), as described previously.[36,37] Fibrillation was conducted at 2 wt % solids at 1500 rpm. The WIS suspension was processed for 4, 6, and 8 passes. The resultant LCNF gels were stored in a cold room (4 °C) until testing. To facilitate discussion, the LCNF samples are labeled as PxxTyytzzNn, with n = 4, 6, 8 denoting passes through the SuperMassColloider.

Chemical Compositional Analyses. For mass balance analyses, the yields of WISs were determined gravimetrically after measuring the moistures of the washed WISs by oven drying aliquot wet WIS samples at 105 °C. The chemical compositions of the WISs were determined by the Analytical Chemistry and Microscopy Laboratory at the USDA Forest Products Laboratory (Madison, WI, USA) using conventional two-step acid hydrolyses, as described previously.[38] In brief, the carbohydrates in WISs were hydrolyzed to monomeric sugars and then analyzed by ion chromatography (ICS-5000, Dionex) with amperometric detection (HPAEC-PAD). The unsolubilized materials were measured gravimetrically. The amounts of ash were first determined from the remains after burning the unsolubilized materials at 560 °C for 3 h. The balances between the amounts of ash and the unsolubilized solids are considered as the Klason lignin. The chemical compositions of the spent liquor were analyzed by an HPLC system (Ultimate 3000, ThermoFisher Scientific), as described previously.[39] Specifically, sugars, furfural, acetic acid, and *p*-TsOH were separated by a BioRad Aminex HPX-87H column (300 mm ×

DOI: 10.1021/acssuschemeng.8b03135
ACS Sustainable Chem. Eng. 2018, 6, 14480−14489

7.8 mm) operated at 60 °C and detected by a refraction index detector (RI-101, Shodex).

Furfural Production from Dissolved Xylan. Collected spent liquors from the three large batch runs were directly used to produce furfural from the dissolved xylan using the *p*-TsOH in the spent liquor to catalyze the dehydration reactions without additional catalysts. The reaction was conducted in a bomb digester heated in a sand bath, as described previously.[40] For each spent liquor, 15 mL was dispensed into a reactor, and then the reactor was sealed, heated to 190 °C in 5 min, and maintained for additional 2.5 min. The reaction was then immediately quenched. The composition of the final liquor was analyzed by HPLC, as discussed above, for sugars and furfural.

Optical Microscopic and Atomic Force Microscopic (AFM) Imaging. The fibrillated WISs and the LNPs in the spent liquor were observed using an optical microscope (Eclipse Ci-L, Nikon, Japan). An aliquot of the fibrillated WIS suspension was first dispensed on an optical microscope slide and then diluted using water. The slide was then covered with an optical glass for direct optical imaging under different magnifications between 2 and 40. The morphologies of LCNFs and LNPs were observed by AFM imaging. Suspensions of LCNFs and LNPs approximately 0.01 wt % were dispersed under sonication, deposited on a mica substrate, and then air-dried at room temperature. The LCNFs were imaged in the vibrating tapping mode on an AFM system (CS-3230, AFM Workshop, CA, USA). The height distributions of LCNFs were obtained by analyzing the AFM topographic images using Image-Pro Plus software (Media Cybernetics, Silver Spring, MD, USA).

LCNF Film Preparation and Mechanical Testing. LCNF films were made using an LCNF suspension at 2 wt % in a filtration system (YT30 142HW, Millipore Corporation, Bedford, MA, USA). A suspension containing 1.62 g (oven dry weight) of LCNFs was poured into the filtration system. The filtration membrane (JVWP14225, Millipore Corporation, USA) had a reported pore size of 0.1 μm supported by filter paper (P2, Fisher Scientific, USA). The filtration tank was pressurized to 3.45 bar. An LCNF film was formed after 30 min of dewatering. The wet LCNF film was taken out and stacked between wax-coated papers. The assembly was then sandwiched between two steel plates, a 23-kg weight was placed on the plates to minimize deformation (changed wax-coated paper frequently to remove water), and the assembly was held at room temperature for 72 h. The films were then taken out and air-dried in a conditioned room under 23 ± 2 °C and 50 ± 5% relative humidity.

The LCNF films were conditioned under 23 ± 2 °C and 50 ± 5% relative humidity for over 40 h prior to mechanical testing. Rectangular shaped testing specimens of 30 mm × 10 mm were cut out from LCNF films. At least five specimens were tested for each film sample. The tension tests were carried out on an Electromechanical Universal Test System (MTS Criterion Model 43). The starting span of the two grips was 25 mm, and the displacement speed was 0.1 mm/s.

Thermogravimetric Analysis (TGA). The thermal stabilities of the original wheat straw and the wheat straw LCNF films were measured using a thermogravimetric analyzer (Pyris 1 TGA, PerkinElmer Inc., Waltham, MA, USA). The samples were heated in the temperature range of 50−600 °C at a heating rate of 10 °C/min under a nitrogen atmosphere with a flow rate of 20 mL/min. All of the samples were dried at 50 °C for 4 h to remove moisture before testing.

RESULTS AND DISCUSSION

Fractionation Mass Balance and Severities. The chemical compositions and yields of the WISs from fractionation runs under different conditions are listed in Table 1 along with glucose, xylose, furfural, and acetic acid concentrations in the spent liquors. Three large batch runs were conducted for the production of LCNFs. Data in parentheses are the component yields in WISs or spent liquors based on the component content in the untreated wheat straw. The results clearly indicate that cellulose dissolutions were low, below 20% for most runs, especially under mild conditions. The very low glucose concentration in the spent liquor suggests that most of the dissolved glucan may well be in the form of oligomers (not analyzed). Degradation products, such as formic acid (Table 1) and WIS yield loss through washing, may have also contributed to the mass imbalance of glucan. High ash yields of 90−110% suggest that all ash (mainly silica) was retained on WIS, which can eliminate precipitation and fouling problems associated with silica in the downstream processing of spent liquor, such as in evaporation for concentration. It also increased the yield of WIS for material production. Furthermore, silica can also increase the thermal stability of WIS, which is important for LCNFs, as will be further discussed later. These issues suggest that reducing silica content using alkaline washing[14] is not necessary and highlight the advantages of acidic fractionation over alkaline processes. Dissolutions of xylan and lignin were substantial under severe fractionation conditions. The maximum lignin and xylan dissolutions were approximately 70 and 80%, respectively. The dissolved xylan was mainly in the form of monomeric xylose under severe conditions, such as xylan dissolution >65%. Xylan mass imbalance under less severe runs was most likely due to xylooligomers that were not analyzed. Furfural production was low, below 3% of the straw xylan content for all the small batch fractionation runs, but increased up to approximately 10% of straw xylan for the large batch runs with extended fractionation times at 90 °C.

In earlier studies of wood fractionation,[41] we developed a reaction kinetic-based combined hydrolysis factor (CHF) to correlate xylan dissolution and cellulose depolymerization for process scale-up.[39,42,43] Here, we applied the same concept for correlating both xylan and lignin dissolution using CHF and CDF (combined delignification factor). The fractions of residual xylan X_R and lignin L_R in WISs can be expressed as

$$X_R = (1 - \theta - \theta_R)e^{-\mathrm{CHF}} + \theta e^{-f\mathrm{CHF}} + \theta_R \quad (1a)$$

$$\mathrm{CHF} = \exp\left(\alpha - \frac{E}{RT} + \beta C\right)Ct \quad (1b)$$

$$L_R = (1 - \theta' - \theta'_R)e^{-\mathrm{CDF}} + \theta' e^{-f'\mathrm{CDF}} + \theta'_R \quad (2a)$$

$$\mathrm{CDF} = \exp\left(\alpha' - \frac{E'}{RT} + \beta' C\right)Ct \quad (2b)$$

where C is the *p*-TsOH molar concentrations (mol/L), R = 8.314 (J/mol/K) is the universal gas content, t is the reaction time in min, and T is the reaction temperature in Kelvin. α, α', β, and β' are adjustable parameters; E and E' are the apparent activation energy (J/mol); and θ and θ' are the initial fraction of slow reacting xylan and lignin, respectively. f and f' are the ratios of the reaction rate between the slow and fast xylan and slow and fast lignin, respectively. θ_R and θ_R' are the residual xylan and lignin, respectively. Excellent fittings of the data in Table 1 were obtained, as shown in Figure 2. This suggests that the desired level of xylan dissolution or delignification can be achieved as long as the required severity CHF or CDF is applied in fractionation, independent of the individual reaction condition. This is important to process scale-up to avoid constraints in practice. For example, for on-farm applications, temperatures below the water boiling point ($T \leq 90$ °C) and low acid concentrations are highly desirable to reduce capital and chemical recovery costs. A long reaction time is tolerable and can be used to compensate for low temperature and low

DOI: 10.1021/acssuschemeng.8b03135
ACS Sustainable Chem. Eng. 2018, 6, 14480−14489

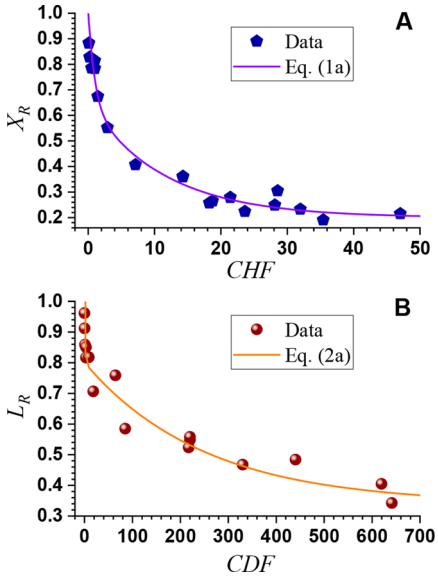

Figure 2. Experimental measured xylan (A) and lignin (B) dissolution under various fractionation severities along with fittings of the data sets to reaction kinetic-based severity factors.

acid loadings. The fitting parameters are listed in Table 2. The substantially lower value of β than β' suggests that

Table 2. List of Fitting Parameters for Eqs 1a, 1b, 2a, and 2b from the Xylan and Lignin Yield Data in Table 1

parameter	unit	xylan	lignin
α, α'	none	21.43	30.34
β, β'	L/mol	0.02	1.04
E, E'	J/mol	70000	95800
θ, θ'	none	0.445	0.462
f, f'	none	0.086	0.004
θ_R, θ_R'	none	0.20	0.34

delignification is much more dependent on *p*-TsOH concentration than the solubilizing hemicelluloses in the present hydrotropic chemistry.

LNPs from Dissolved Lignin. The dissolved lignin in the spent *p*-TsOH liquors is in the form of LNPs. AFM images of the spent liquors from the three large batch runs indicate that a severer condition resulted in LNPs with smaller particles, as shown in Figure 3A,B,C. This is in agreement with our previous study.[44] AFM-measured LNP height distribution (Figure 3D) indicates a severer condition also resulted in thicker LNPs with a mean height of approximately 14 nm for the P35T90t120 compared with 6 nm for P15T90t120. As reported previously, these LNPs are not spherical, as evidenced by the diameters being on the order of 30−100 nm while the heights were on the order of nanometers obtained from AFM measurements.[28,45]

Furfural Produced from Dissolved Xylan. Dehydration of dissolved xylan in spent liquor catalyzed by the *p*-TsOH in the liquor resulted in a large amount of furfural, as listed in Table 3. Xylose was mostly consumed (comparing xylose in feed spent liquor in Table 1). Furfural yields (including those produced in the fractionation step) based on the amount of dissolved xylan reached over 55% in a batch reactor, which is considered high because batch operation is always accompanied by side reactions, such as condensation with furfural

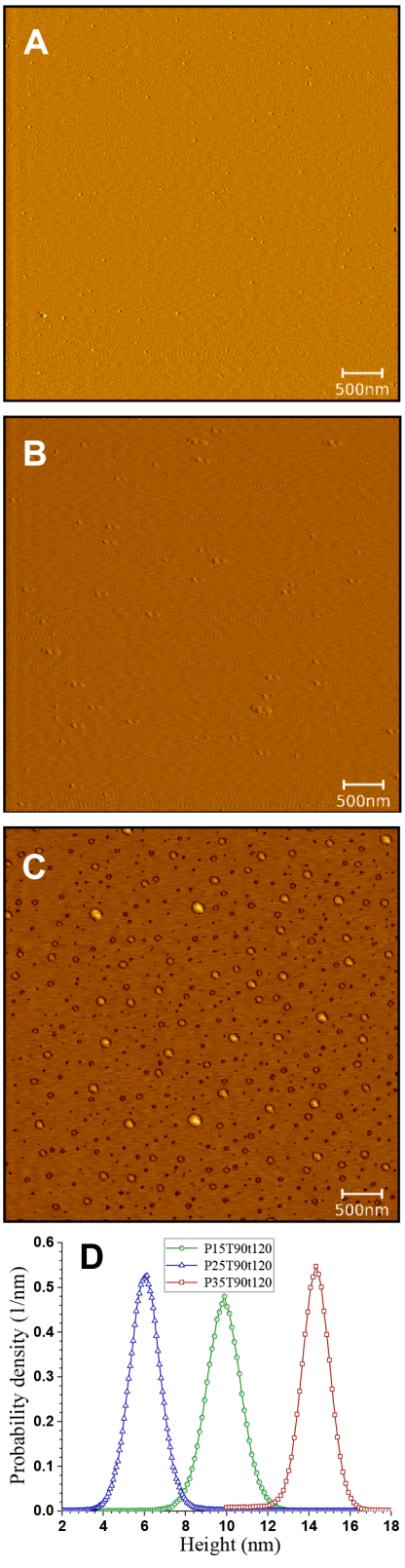

Figure 3. (A−C) Scale bars = 100 μm. Atomic force microscopic (AFM) images of LNPs from large batch runs under different *p*-TsOH concentrations, P15T90t120 (A), P25T90t120 (B), and P35T80t120 (C). (D) AFM-measured height distributions of LNPs from the runs in (A−C).

itself, glucose, xylose, and other compounds.[46] Simply using batch with distillation can substantially improve the furfural

DOI: 10.1021/acssuschemeng.8b03135
ACS Sustainable Chem. Eng. 2018, 6, 14480−14489

Table 3. Xylose and Furfural Concentrations in the Final Spent Liquors after Direct Dehydration of the Spent Liquors (Feed) Collected from the Three Large Batch Runs Using the *p*-TsOH in the Feed Liquor as the Catalyst[a]

spent liquor	*p*-TsOH[b] (g/L)	glucose (g/L)	xylose (g/L)	furfural (g/L)	furfural yield[c] (%)	HMF (g/L)	formic acid (g/L)	acetic acid (g/L)
P15T90t120	138	0.64	1.06	2.96	44.8	0.006	0.35	0.43
P25T90t120	268	0.51	0.57	3.90	57.0	0.003	0.66	0.49
P35T90t120	337	0.06	0.44	3.68	52.7	0.001	0.98	0.64

[a]Xylose and furfural concentrations in the feed spent liquors are listed in Table 1. [b]Averages of the measured *p*-TsOH concentrations in the feed spent liquor and its corresponding final spent liquor. [c]Calculated using the measured furfural from the final liquor (including furfural production in the fractionation process) as the percentage of the theoretical achievable furfural from the amount of dissolved xylan in the spent liquor.

yield.[40,47] Therefore, the furfural yield can be improved in actual on-farm operations using various process modifications.

LCNFs Produced from WISs. Our earlier study indicated that partial delignification is necessary for improving nanofibrillation to reduce mechanical energy input.[17] To produce LCNF using raw wheat straw directly, our main interest is to examine the effect of delignification on mechanical fibrillation, especially because delignification is highly dependent on acid concentration, on the basis of the fractionation results discussed above. We chose to use different *p*-TsOH concentrations to vary the degree of delignification, while keeping the variations in xylan dissolution minimal. As shown in Table 1, the three large batch runs with *p*-TsOH concentration of 15, 25, and 35 wt % were all carried out at T = 90 °C for 120 min and resulted in delignification of approximately 24, 48, and 66%, with approximately the same amounts of xylan dissolution of 74, 77, and 78%, respectively. Optical microscopy analyses indicated that substantial amounts of fibers remained after eight passes of SMC grinding for P15T90t120 WIS, which had 24% delignification (Figure 4A–C). The amount of fibers decreased, and fibrils became finer with increasing delignification (comparing the three columns in Figure 4). With 66% delignification, the WIS from P35T90t120 was substantially fibrillated even at six passes through SMC (Figure 4H,I). For more detailed examination of the nanofibrils, the fibrillated samples from P25T90t120 and P35T90t120 were analyzed using AFM (the samples from P15T90t120 were not fine enough for AFM imaging). Increasing delignification resulted in finer fibrils under the same number of passes of SMC grinding, as clearly shown by the AFM images (Figure 5A,C). For P35T90t120, increasing SMC grinding to eight passes resulted in thinner fibrils (Figure 5D) with less entanglement (Figure 5B,C). Some free lignin particles were separated from the nanofibrils during SMC grinding and can be clearly seen from the AFM images (Figure 5A,B,C).

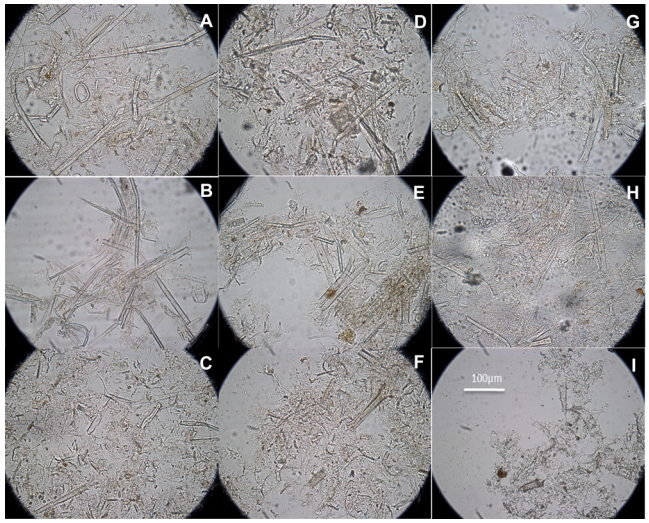

Figure 4. Optical microscopic images of fibrils after N = 4 (top row), 6 (middle row), and 8 (bottom row) passes of SMC grinding of wheat straw WISs from different fractionation conditions. (A–C) P15T90t120, (D–F) P25T90t120, and (G–I) P35T90t120. Scale bar = 100 μm is for all images.

The degrees of delignification also affected the energy input for SMC grinding. At the low delignification level of 24%, energy consumption after eight passes was high at 20.5 MJ/kg, similar to that reported using a bleached Eucalyptus kraft pulp (lignin content ≈ 0) after 2 h of grinding[48] (approximately eight passes). Increased delignification substantially reduced the energy input to approximately 12 MJ/kg for both WISs from P25T90t120 and P35T90t120, with delignification of 48 and 66%, respectively. This indicates delignification of over approximately 50% did not show substantial savings in the energy input for mechanical fibrillation (Figure S1). Energy input was linearly dependent on the number of passes through the SMC (or time), agreeing with our earlier studies.[48]

p-TsOH fractionation enriched the silica content, which substantially improved the overall thermal stability of the LCNFs, as shown in Figure 6A, despite the removal of lignin. Onset thermal degradation occurred at a much lower temperature for the raw wheat straw than for the fractionated straw samples (Figure 6A). Due to measurement uncertainties, the data cannot discern the difference among the three fractionated straw samples. The degradation of LCNF showed two steps, and the first step was associated with lignocelluloses in the dW/dt plot (Figure 6B). It appears that the peak intensity in the first step is inversely proportional to the lignin content of the samples. For example, the sample from P35T90t120 with the lowest lignin content had the highest peak or the most rapid reduction in weight; the sample from the P15T90t120 with the highest lignin content (higher than the raw wheat straw due to the removal of hemicelluloses) had the lowest peak or the slowest reduction in weight. The second step peak in the dW/dt plot was associated with the degradation of inorganic silica, similar to that observed in silica-containing composites.[49] *p*-TsOH enriched the silica content and is therefore advantageous for improving the thermal stability of resultant materials, which are suitable for composite applications.

Mechanical Properties of Wheat Straw LCNFs from *p*-TsOH Fractionation. LCNF films were used to test the mechanical properties of the LCNFs. The results indicate that specific tensile strengths over 100 and up to 140 kN·m/kg were achieved with various degrees of delignification and the extents of mechanical fibrillation (passes through SMC), which is substantially higher than the approximately 75 kN·m/kg

DOI: 10.1021/acssuschemeng.8b03135
ACS Sustainable Chem. Eng. 2018, 6, 14480–14489

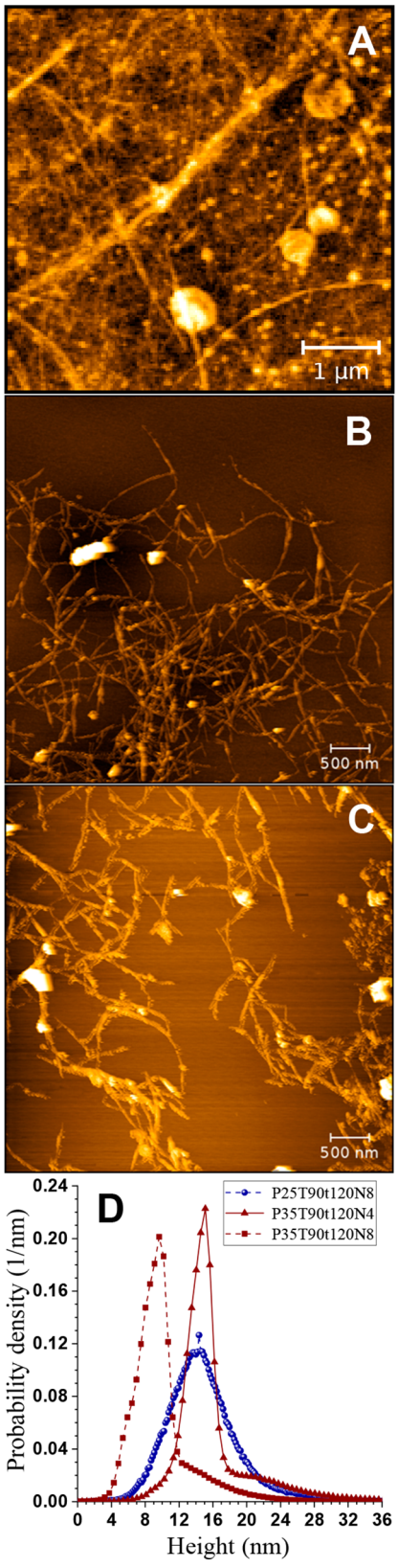

Figure 5. AFM analyses of LCNFs from *p*-TsOH-fractionated WISs after varied passes through SMC grinding. (A) P25T90t120N8, (B) P35T90t120N4, and (C) P35T90t120N8. (D) AFM-measured LCNF height distributions.

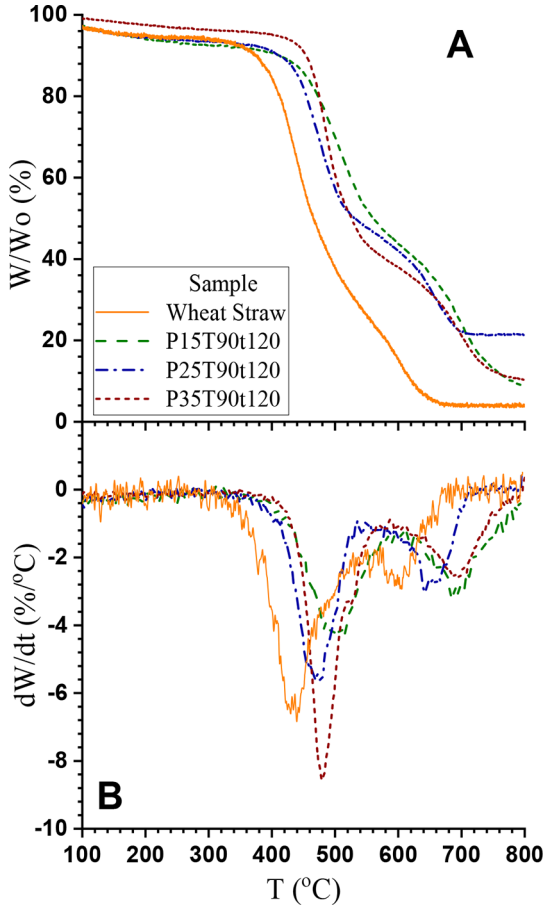

Figure 6. TGA of the raw wheat straw and films of LCNFs from *p*-TsOH-fractionated wheat straw WISs.

achieved by a CNF film made from a bleached Eucalyptus kraft pulp after 7 h through the SMC.[50] In general, increasing the extent of mechanical fibrillation increased specific tensile strength, as shown in Figure 7A. Increasing the amount of delignification also increased the specific tensile strength. Both of these two phenomena were most likely due to the increased hydrogen bonding because of the increased specific bonding surface area through fibrillation and delignification. The maximal tensile strength of approximately 140 kN·m/kg for P35T90t120N8 with 66% delignification, or a lignin content of approximately 12%, was higher than 120 kN·m/kg for a CNF film from a bleached Eucalyptus kraft pulp after 47 passes through a microfluidizer.[50] It is also higher than 97 kN·m/kg for an LCNF film of equivalent lignin content (13.5%) produced from an organosolv spruce pulp through homogenization.[51] Overall, the tensile strength of the present wheat straw nanofibril films is at least on par with those produced from wood nanofibrils with various lignin content.[52]

The specific stress and strain data were fitted using a hyperbolic tangent function to obtain a specific tensile modulus of the LCNF films. The results show that specific moduli were fairly constant at approximately 5 MN·m/kg under the processing conditions studied (Figure 7B), which are lower than CNF films made from bleached Eucalyptus fibers[50] and organosolv spruce fibers.[51] The tensile strains obtained in this study were as high as 5% (Figure 7C), higher than those nanofibril films produced from wood fibers with various lignin content.[52] Perhaps lignin, especially those free lignin nanoparticles (Figure 5A–C), in LCNFs resulted in film

DOI: 10.1021/acssuschemeng.8b03135
ACS Sustainable Chem. Eng. 2018, 6, 14480−14489

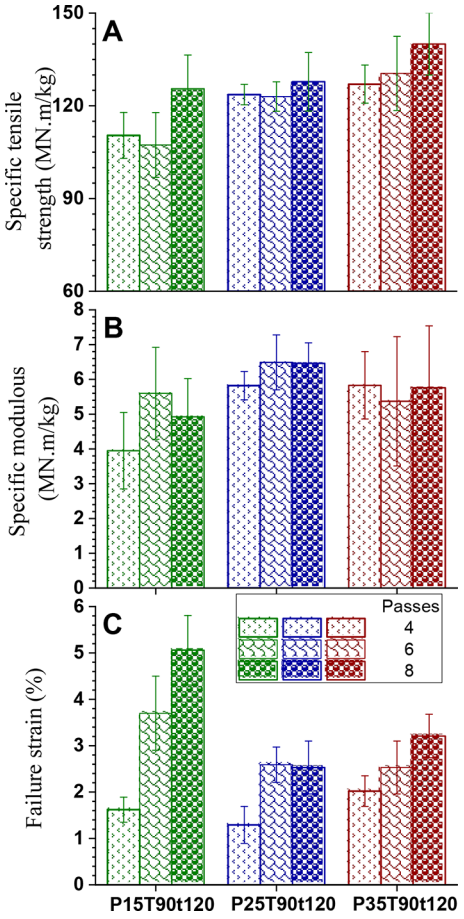

Figure 7. Specific tensile strength (A), specific tensile modulus (B), and failure strain (C) of LCNF films made from *p*-TsOH-fractionated wheat straw at different severities with a varied degree of mechanical fibrillation (passes through SMC).

flexibility. Both high strain and tensile strength are favorable to increased film toughness.

CONCLUSIONS

This study demonstrated the potential for sustainable and economic valorization of wheat straw, an agriculture residue, through a low-temperature fractionation process using an acid hydrotrope, *p*-TsOH. Wheat straw can be fractionated into a cellulose-rich solid fraction and a dissolved lignin stream under temperatures below the water boiling point. The silica in the wheat straw was fully retained on the solid fraction, which not only increased solid yield but also increased thermal stability. The solid fraction can be used to produce LCNFs after mechanical fibrillation. Films made from the resulting LCNFs had great mechanical properties, with specific tensile strength over 120 kN·m/kg, even with a lignin content as high as 22%. The films also had good failure strains of approximately 1.5% or higher. The dissolved lignin can be easily precipitated as LNPs, another wood-based nanomaterial, simply through dilution with water. The dissolved xylan can be dehydrated into furfural using the *p*-TsOH in the spent liquor without additional catalysts or chemicals. The low-temperature fractionation process eliminates the need for high-cost pressure vessels and is suitable for on-farm applications.

ASSOCIATED CONTENT

Supporting Information

The Supporting Information is available free of charge on the ACS Publications website at DOI: 10.1021/acssuschemeng.8b03135.

Energy inputs for fibrillation of *p*-TsOH fractionated wheat straw WISs under different conditions using SMC for various passes, images of LCNF films from *p*-TsOH fractionated wheat straw under different severities after eight passes through the SuperMassColloider, examples of fittings of specific tensile stress and strain data using a hyperbolic tangent function, $\sigma = a \times \text{Tan H}[b(\varepsilon - c)]$, and FTIR analyses of the three LCNF samples obtained under different fractionation severities along with the untreated wheat straw (PDF)

AUTHOR INFORMATION

Corresponding Author

*E-mail: jzhu@fs.fed.us; Tel.: +1-608 231 9520.

ORCID

Rendang Yang: 0000-0002-5928-9852

J.Y. Zhu: 0000-0002-5136-0845

Notes

The authors declare the following competing financial interest(s): Zhu and Glesiner are co-inventors of the p-TsOH fractionation process.

ACKNOWLEDGMENTS

This work was partially supported by the USDA Forest Service and a Chinese Scholarship Council that made the visiting appointment of Q.M. at the USDA Forest Products Laboratory (FPL) possible. We acknowledge Prof. Troy Runge of the University of Wisconsin−Madison for his generous assistance in mechanical testing using his equipment, and Philip Walsh (FPL), Weiqi Leng (FPL), and Fred Matt (FPL) for conducting thermogravimetric and chemical composition analyses.

REFERENCES

(1) Perlack, R. D.; Stokes, B. J. *DOE. 2011. U.S. Billion-Ton Update: Biomass Supply for a Bioenergy and Bioproducts Industry*; Oakridge National Laboratory: Oak Ridge, TN, 2011.

(2) Bakker, R.; Elbersen, W.; Poppens, R.; Lesschen, J. P. *Rice straw and wheat straw. Potential feedstocks for the biobased economy*; Report for the NL Agency Ministry of Economic Affairs, The Netherlands, 2013.

(3) Zhou, X.; Wang, F.; Hu, H.; Yang, L.; Guo, P.; Xiao, B. Assessment of sustainable biomass resource for energy use in China. *Biomass Bioenergy* **2011**, *35* (1), 1−11.

(4) Montero, G.; García, C.; Coronado, M. A.; Toscano, L.; Stoytcheva, M.; Torres, R.; Vazquez, A. M.; Montes, D. G. SWOT analysis applied to wheat straw utilization as a biofuel in Mexico. In *Frontiers in Bioenergy and Biofuels*; Jacob-Lopes, E., Ed.; London, UK, 2017; pp 483−493.

(5) Doyle, C. J.; Mason, V. C.; Baker, R. D. Straw disposal and utilization: An economic evaluation of the alternative end-uses for wheat straw in the UK. *Biol. Wastes* **1988**, *23*, 39−56.

(6) Zhang, P.; Wei, T.; Jia, Z.; Han, Q.; Ren, X.; Li, Y. Effects of straw incorporation on soil organic matter and soil water-stable aggregates content in semiarid regions of Northwest China. *PLoS One* **2014**, *9* (3), e92839.

DOI: 10.1021/acssuschemeng.8b03135
ACS Sustainable Chem. Eng. 2018, 6, 14480−14489

(7) Xie, L.; Liu, M.; Ni, B.; Wang, Y. Utilization of wheat straw for the preparation of coated controlled-release fertilizer with the function of water retention. *J. Agric. Food Chem.* **2012**, *60* (28), 6921−6928.
(8) Xie, W.; Zhang, Y.; Wu, T.; Wu, L.; Li, X.; Ouyang, Z. Effects of straw application on coastal saline topsoil salinity and wheat yield trend. *Soil Tillage Res.* **2017**, *169*, 1−6.
(9) Khan, A.; De Jong, W.; Jansens, P.; Spliethoff, H. Biomass combustion in fluidized bed boilers: potential problems and remedies. *Fuel Process. Technol.* **2009**, *90* (1), 21−50.
(10) Zeng, X.; Ma, Y.; Ma, L. Utilization of straw in biomass energy in China. *Renewable Sustainable Energy Rev.* **2007**, *11* (5), 976−987.
(11) Niu, Y.; Tan, H.; Hui, S. e. Ash-related issues during biomass combustion: Alkali-induced slagging, silicate melt-induced slagging (ash fusion), agglomeration, corrosion, ash utilization, and related countermeasures. *Prog. Energy Combust. Sci.* **2016**, *52*, 1−61.
(12) Ma, Q.; Han, L.; Huang, G. Evaluation of different water-washing treatments effects on wheat straw combustion properties. *Bioresour. Technol.* **2017**, *245*, 1075−1083.
(13) Bian, H.; Gao, Y.; Yang, Y.; Fang, G.; Dai, H. Improving cellulose nanofibrillation of waste wheat straw using the combined methods of prewashing, p-toluenesulfonic acid hydrolysis, disk grinding, and endoglucanase post-treatment. *Bioresour. Technol.* **2018**, *256*, 321−327.
(14) Alemdar, A.; Sain, M. Isolation and characterization of nanofibers from agricultural residues - Wheat straw and soy hulls. *Bioresour. Technol.* **2008**, *99* (6), 1664−1671.
(15) Espinosa, E.; Tarres, Q.; Delgado-Aguilar, M.; Gonzalez, I.; Mutje, P.; Rodríguez, A. Suitability of wheat straw semichemical pulp for the fabrication of lignocellulosic nanofibres and their application to papermaking slurries. *Cellulose* **2016**, *23* (1), 837−852.
(16) Liu, Q.; Lu, Y.; Aguedo, M.; Jacquet, N.; Ouyang, C.; He, W.; Yan, C.; Bai, W.; Guo, R.; Goffin, D.; Song, J.; Richel, A. Isolation of High-Purity Cellulose Nanofibers from Wheat Straw through the Combined Environmentally Friendly Methods of Steam Explosion, Microwave-Assisted Hydrolysis, and Microfluidization. *ACS Sustainable Chem. Eng.* **2017**, *5* (7), 6183−6191.
(17) Hoeger, I. C.; Nair, S. S.; Ragauskas, A. J.; Deng, Y.; Rojas, O. J.; Zhu, J. Y. Mechanical deconstruction of lignocellulose cell walls and their enzymatic saccharification. *Cellulose* **2013**, *20* (2), 807−818.
(18) Jiang, C.; He, H.; Jiang, H.; Ma, L.; Jia, D. Nano-lignin filled natural rubber composites: Preparation and characterization. *eXPRESS Polym. Lett.* **2013**, *7* (5), 480−493.
(19) Nair, S. S.; Sharma, S.; Pu, Y.; Sun, Q.; Pan, S.; Zhu, J. Y.; Deng, Y.; Ragauskas, A. J. High shear homogenization of lignin to nanolignin and thermal stability of nanolignin-polyvinyl alcohol blends. *ChemSusChem* **2014**, *7* (12), 3513−3520.
(20) Ago, M.; Huan, S.; Borghei, M.; Raula, J.; Kauppinen, E. I.; Rojas, O. J. High-throughput synthesis of lignin particles (∼30 nm to ∼ 2 μm) via aerosol flow reactor: Size fractionation and utilization in pickering emulsions. *ACS Appl. Mater. Interfaces* **2016**, *8* (35), 23302−23310.
(21) Qian, Y.; Zhang, Q.; Qiu, X.; Zhu, S. CO_2-responsive diethylaminoethyl-modified lignin nanoparticles and their application as surfactants for CO_2/N_2-switchable Pickering emulsions. *Green Chem.* **2014**, *16* (12), 4963−4968.
(22) Figueiredo, P.; Ferro, C.; Kemell, M.; Liu, Z.; Kiriazis, A.; Lintinen, K.; Florindo, H. F.; Yli-Kauhaluoma, J.; Hirvonen, J.; Kostiainen, M. A.; Santos, H. A. Functionalization of carboxylated lignin nanoparticles for targeted and pH-responsive delivery of anticancer drugs. *Nanomedicine* **2017**, *12* (21), 2581−2596.
(23) Tortora, M.; Cavalieri, F.; Mosesso, P.; Ciaffardini, F.; Melone, F.; Crestini, C. Ultrasound driven assembly of lignin into microcapsules for storage and delivery of hydrophobic molecules. *Biomacromolecules* **2014**, *15* (5), 1634−1643.
(24) Frangville, C.; Rutkevičius, M.; Richter, A. P.; Velev, O. D.; Stoyanov, S. D.; Paunov, V. N. Fabrication of environmentally biodegradable lignin nanoparticles. *ChemPhysChem* **2012**, *13* (18), 4235−4243.
(25) Lievonen, M.; Valle-Delgado, J. J.; Mattinen, M.-L.; Hult, E.-L.; Lintinen, K.; Kostiainen, M. A.; Paananen, A.; Szilvay, G. R.; Setala, H.; Osterberg, M. A simple process for lignin nanoparticle preparation. *Green Chem.* **2016**, *18* (5), 1416−1422.
(26) Myint, A. A.; Lee, H. W.; Seo, B.; Son, W. S.; Yoon, J.; Yoon, T. J.; Park, H. J.; Yu, J.; Lee, Y. W.; Yoon, J. One pot synthesis of environmentally friendly lignin nanoparticles with compressed liquid carbon dioxide as an antisolvent. *Green Chem.* **2016**, *18* (7), 2129−2146.
(27) Richter, A. P.; Bharti, B.; Armstrong, H. B.; Brown, J. S.; Plemmons, D.; Paunov, V. N.; Stoyanov, S. D.; Velev, O. D. Synthesis and characterization of biodegradable lignin nanoparticles with tunable surface properties. *Langmuir* **2016**, *32* (25), 6468−6477.
(28) Chen, L.; Dou, J.; Ma, Q.; Li, N.; Wu, R.; Bian, H.; Yelle, D. J.; Vuorinen, T.; Fu, S.; Pan, X.; Zhu, J. Y. Rapid and near-complete dissolution of wood lignin at ⩽ 80 °C by a recyclable acid hydrotrope. *Sci. Adv.* **2017**, *3* (9), e1701735.
(29) Iakovlev, M.; van Heiningen, A. Efficient fractionation of spruce by SO2-ethanol-water treatment: Closed mass balances for carbohydrates and sulfur. *ChemSusChem* **2012**, *5* (8), 1625−1637.
(30) Luterbacher, J. S.; Rand, J. M.; Alonso, D. M.; Han, J.; Youngquist, J. T.; Maravelias, C. T.; Pfleger, B. F.; Dumesic, J. A. Nonenzymatic sugar production from biomass using biomass-derived γ-valerolactone. *Science* **2014**, *343* (6168), 277−280.
(31) Brandt, A.; Ray, M. J.; To, T. Q.; Leak, D. J.; Murphy, R. J.; Welton, T. Ionic liquid pretreatment of lignocellulosic biomass with ionic liquid-water mixtures. *Green Chem.* **2011**, *13* (9), 2489−2499.
(32) Morais, A. R. C.; Pinto, J. V.; Nunes, D.; Roseiro, L. B.; Oliveira, M. C.; Fortunato, E.; Bogel-Łukasik, R. Imidazole: Prospect Solvent for Lignocellulosic Biomass Fractionation and Delignification. *ACS Sustainable Chem. Eng.* **2016**, *4* (3), 1643−1652.
(33) Anugwom, I.; Eta, V.; Virtanen, P.; Maki-Arvela, P.; Hedenstrom, M.; Hummel, M.; Sixta, H.; Mikkola, J. P. Switchable ionic liquids as delignification solvents for lignocellulosic materials. *ChemSusChem* **2014**, *7* (4), 1170−1176.
(34) Morais, A. R. C.; Da Costa Lopes, A. M.; Bogel-Łukasik, R. Carbon dioxide in biomass processing: Contributions to the green biorefinery concept. *Chem. Rev.* **2015**, *115* (1), 3−27.
(35) Zhu, J. Y.; Chandra, M. S.; Gu, F.; Gleisner, R.; Reiner, R.; Sessions, J.; Marrs, G.; Gao, J.; Anderson, D. Using sulfite chemistry for robust bioconversion of Douglas-fir forest residue to bioethanol at high titer and lignosulfonate: A pilot-scale evaluation. *Bioresour. Technol.* **2015**, *179*, 390−397.
(36) Qin, Y.; Qiu, X.; Zhu, J. Y. Understanding longitudinal wood fiber ultra-structure for producing cellulose nanofibrils using disk milling with dilute acid prehydrolysis. *Sci. Rep.* **2016**, *6*, 35602.
(37) Hu, C.; Zhao, Y.; Li, K.; Zhu, J. Y.; Gleisner, R. Optimizing cellulose fibrillation for the production of cellulose nanofibrils by a disk grinder. *Holzforschung* **2015**, *69* (8), 993−1000.
(38) Luo, X.; Gleisner, R.; Tian, S.; Negron, J.; Horn, E.; Pan, X. J.; Zhu, J. Y.; Zhu, W. Evaluation of mountain beetle infested lodgepole pine for cellulosic ethanol production by SPORL pretreatment. *Ind. Eng. Chem. Res.* **2010**, *49* (17), 8258−8266.
(39) Zhou, H.; Zhu, J. Y.; Luo, X.; Leu, S.-Y.; Wu, X.; Gleisner, R.; Dien, B. S.; Hector, R. E.; Yang, D.; Qiu, X.; Horn, E.; Negron, J. Bioconversion of beetle-killed lodgepole pine using SPORL: Process scale-up design, lignin coproduct, and high solids fermentation without detoxification. *Ind. Eng. Chem. Res.* **2013**, *52* (45), 16057−16065.
(40) Ji, H.; Chen, L.; Zhu, J. Y.; Gleisner, R.; Zhang, X. Reaction kinetics based optimization of furfural production from corncob using a fully recyclable solid acid. *Ind. Eng. Chem. Res.* **2016**, *55* (43), 11253−11259.
(41) Zhu, W.; Houtman, C. J.; Zhu, J. Y.; Gleisner, R.; Chen, K. F. Quantitative predictions of bioconversion of aspen by dilute acid and SPORL pretreatments using a unified combined hydrolysis factor (CHF). *Process Biochem.* **2012**, *47*, 785−791.
(42) Wang, R.; Chen, L.; Zhu, J. Y.; Yang, R. Tailored and integrated production of carboxylated cellulose nanocrystals (CNC) with

DOI: 10.1021/acssuschemeng.8b03135
ACS Sustainable Chem. Eng. 2018, 6, 14480−14489

nanofibrils (CNF) through maleic acid hydrolysis. *ChemNanoMat* **2017**, *3* (5), 328−335.
(43) Zhou, H.; Zhu, J. Y.; Gleisner, R.; Qiu, X.; Horn, E. High titer ethanol and lignosulfonate productions from SPORL pretreated poplar at pilot-scale. *Front. Energy Res.* **2015**, *3*, 16.
(44) Ma, Q.; Chen, L.; Wang, W.; Yang, R.; Zhu, J. Y. Direct production of lignin nanoparticles (LNPs) from wood using p-toluenesulfonic acid in an aqueous system at 80°C: Characterization of LNP morphology, size, and surface charge. *Holzforschung* **2018**, *72*, 1.
(45) Bian, H.; Chen, L.; Gleisner, R.; Dai, H.; Zhu, J. Y. Producing wood-based nanomaterials by rapid fractionation of wood at 80 °C using a recyclable acid hydrotrope. *Green Chem.* **2017**, *19*, 3370−3379.
(46) Weingarten, R.; Cho, J.; Conner, W. C., Jr; Huber, G. W. Kinetics of furfural production by dehydration of xylose in a biphasic reactor with microwave heating. *Green Chem.* **2010**, *12* (8), 1423−1429.
(47) Mandalika, A.; Runge, T. Enabling integrated biorefineries through high-yield conversion of fractionated pentosans into furfural. *Green Chem.* **2012**, *14* (11), 3175−3184.
(48) Wang, Q. Q.; Zhu, J. Y.; Gleisner, R.; Kuster, T. A.; Baxa, U.; McNeil, S. E. Morphological development of cellulose fibrils of a bleached eucalyptus pulp by mechanical fibrillation. *Cellulose* **2012**, *19* (5), 1631−1643.
(49) Peng, Z.; Kong, L. X. A thermal degradation mechanism of polyvinyl alcohol/silica nanocomposites. *Polym. Degrad. Stab.* **2007**, *92* (6), 1061−1071.
(50) Wang, Q. Q.; Zhu, J. Y.; Considine, J. M. Strong and optically transparent films prepared using cellulosic solid residue (CSR) recovered from cellulose nanocrystals (CNC) production waste stream. *ACS Appl. Mater. Interfaces* **2013**, *5* (7), 2527−2534.
(51) Rojo, E.; Peresin, M. S.; Sampson, W. W.; Hoeger, I. C.; Vartiainen, J.; Laine, J.; Rojas, O. J. Comprehensive elucidation of the effect of residual lignin on the physical, barrier, mechanical, and surface properties of nanocellulose films. *Green Chem.* **2015**, *17*, 1853−1866.
(52) Spence, K. L.; Venditti, R. A.; Habibi, Y.; Rojas, O. J.; Pawlak, J. J. The effect of chemical composition on microfibrillar cellulose films from wood pulps: Mechanical processing and physical properties. *Bioresour. Technol.* **2010**, *101* (15), 5961−5968.

DOI: 10.1021/acssuschemeng.8b03135
ACS Sustainable Chem. Eng. 2018, 6, 14480−14489